Sigma J Eng Nat Sci, Vol. 43, No. 6, pp. 1943−1956, December, 2025

Sigma Journal of Engineering and Natural Sciences
Web page info: https://sigma.yildiz.edu.tr
DOI: 10.14744/sigma.2025.00092

Research Article

Biosynthesis of silver nanoparticles using aerial parts of *Cardaria draba* L.: Phytochemical analysis, characterization, evaluation of antibacterial, cytotoxic on human colon cancer cell line properties and enzyme inhibitory potentials

Özlem BAKIR BOĞA[1,*], Esabi BAŞARAN KURBANOĞLU[1]

[1]*Department of Biology, Faculty of Science, Ataturk University, Erzurum, 25240, Türkiye*

ARTICLE INFO

Article history
Received: 20 December 2024
Revised: 21 March 2025
Accepted: 11 May 2025

Keywords:
Cardaria Draba L.; Colorectal Adenocarcinoma Cancer; Enzyme İnhibition; Green Synthesis; Silver Nanoparticles

ABSTRACT

Green nanoparticle synthesis using plant methods has garnered considerable interest from scientific groups because of its benefits, including being environmentally benign and time-efficient. *Cardaria draba* L., aqueous extract was used in this work to create silver nanoparticles in an environmentally friendly manner. SEM, EDX, XRD, UV-VIS, and FT-IR were all employed in the characterization investigations. Silver nanoparticles were measured to have a mean particle size of 41 nm. It was observed that silver nanoparticles' absorbance increased at 460 nm in the UV-Vis spectrum. Using EDX analysis, it was discovered that 78.11% of the scanned region contained Ag. GC-MS analysis revealed that the allyl isothiocyanate compound was responsible for 74.07 percent of the total weight of the plant extract. In the LC-MS/MS results of *Cardaria draba*, vitexin is the phenolic compound found in the highest amount with 8561.6281 ng/mL. Its antibacterial properties have been investigated on various microorganisms that cause infection, which suggests it may offer alternative solutions for treating infectious diseases. The MTT technique was used to assess the cytotoxic effects of silver nanoparticles on human colon cancer cell lines. In the human colon cancer cell line, studies have shown that the administration of silver nanoparticles increased cell death. It was determined that silver nanoparticles synthesized from *C.draba* have high inhibitory effects on the enzymes urease (44.64%) and collagenase (35.55%). This study did not show any LOX enzyme inhibition activity. It has been revealed that these enzyme potential are of interest as a research area in the pharmaceutical and cosmetic industries.

Cite this article as: Bakir Boğa Ö, Başaran Kurbanoğlu E. Biosynthesis of silver nanoparticles using aerial parts of *Cardaria draba* L.: Phytochemical analysis, characterization, evaluation of antibacterial, cytotoxic on human colon cancer cell line properties and enzyme inhibitory potentials. Sigma J Eng Nat Sci 2025;43(6):1943−1956.

***Corresponding author.**
*E-mail address: ozlembakir@atauni.edu.tr

This paper was recommended for publication in revised form by Editor-in-Chief Ahmet Selim Dalkilic

Published by Yıldız Technical University Press, İstanbul, Turkey
© Author. This is an open access article under the CC BY-NC license (http://creativecommons.org/licenses/by-nc/4.0/).

INTRODUCTION

The field of nanotechnology is the most dynamic research area in material sciences, and the synthesis of nanoparticles is increasing significantly worldwide. Nanotechnology is a field in which nanomaterials are produced using particles in the <100 nm size range . As a result of the research and discoveries, AgNPs (silver nanoparticles) have garnered interest due to their chemical, physical, and biological properties and their widespread use in both industrial and health fields [1]. In addition, the synthesis of metal nanoparticles, such as AgNPs, which exhibit antioxidant and antimicrobial activities has gained importance in biochemical applications [2]. Recently, many studies have proven that plants can act as effective precursors for metal nanoparticle synthesis. These studies have enabled people to realize new production models in an environmentally friendly way despite the pollution they experience in modern times [3]. The green synthesis method has become quite popular in recent years [4]. In the green synthesis method, biological resources such as plants, bacteria, fungi, and algae, among others, are used as reducing agents to form nanoparticles. Thus, high costs and waste generation are prevented by using materials that are suitable for large-scale commercial production, non-toxic, highly stable, environmentally friendly, and inexpensive. Since the plants involved in green synthesis form compounds containing functional groups such as phenolics and flavonoids, the nanoparticles formed by the reduction of these compounds have antioxidant, antibacterial and catalytic properties [5]. Thus, metal oxide nanoparticles produced via green synthesis are applied in many areas such as the enzyme industry, drug delivery systems, and biomedical and pharmaceutical applications [6, 7, 8].

Cardaria draba (Brassicaceae), known as watercress, is an annual herbaceous plant. Animal feed and treatment: the aboveground parts are fed to animals. The leaves are crushed and applied externally to wounds on the heads of animals infected with anthrax; these leaves are changed several times a day, and it is said that this method heals the wound. The aboveground parts are used as food [9, 10, 11], animal feed [12], a pain reliever [11], a sedative, a wound healer [13], a diuretic, and to remove kidney stones [14]. Although *C. draba* prefers alkaline conditions, it can be found in different soil types with adequate moisture, growing in a wide variety of habitats such as shady open spaces, meadows, fields, croplands, grasslands, and roadsides [15]. *C. draba* has been used against various ailments in the past [16]. The aerial parts of *C. draba* contain alkaloids, saponins, flavonoids, terpenoids, tannins, triterpenoids, and leukoanthocyanins. The essential oil contains o-xylene, p-xylene, nonane, styrene, hexane-3,3,4-trimethyl, octane-2,6-dimethyl, heptane, 3-methyl-2-ethyl, decane, and nonan-4-methyl; it is also registered to have nonane-2-methyl, benzene-1-ethyl-2-methyl, cyclohexene-2-methylpropyl, mesitylene, dodecane, limonene, benzenacetaldehyde, tetradecane, and 5-(methylthio)-pentane compounds. While Kaempferol, quercetin and isorhamnetin are the most abundant compounds in the ethanolic extract of the leaves, the most abundant compounds in the ethanolic extract of the seeds are ellagic acid, sinapic acid, p-coumaric acid and caffeic acid [17, 18]. it is also used against kidney stones due to its expectorant and diuretic effects. *C. draba* seeds and leaves have expectorant and laxative effects [19]. It has been used as a carminative and has antiscorbutic activity [20]. In the past, *C. draba,* as one of the existing traditional medicines, has been used against a wide variety of ailments. For example, it has been used in anti-inflammatory, anticancer, antimicrobial, antioxidant, hypoglycemic, and other areas.

The selection of *C. draba* was made for a number of reasons. The antibacterial properties of medicinal plants are one of their beneficial aspects, and examining these properties is crucial for understanding their potential applications. Many bacteria have developed resistance to antibiotics as a result of the increased usage of antibiotics. Therefore, the search for novel sources of antibacterials is crucial. Using medicinal herbs is a top priority for this reason. Furthermore, compared to medicines, their potent antibacterial chemicals provide less risk to the user. Medicinal herbs have long been regarded as chemical alternatives because of their affordability, ease of use, low toxicity, and fewer adverse effects. Medicinal plants have made many contributions to the literature in the search for antibacterial sources and in the field of nanotechnology. Silver nanoparticles made with *C.origanifolium* extract were found to have antimicrobial properties that were superior to those of synthetic antimicrobial medications by inhibiting the growth of *Pseudomonas aeruginosa* bacteria, and *Candida albicans* pathogenic fungus [21]. Silver nanoparticles (AgNP) synthesized using extract of *Amygdalus spinosissima* were studied for their antibacterial, antioxidant, anticancer, and apoptotic properties. It was shown that AgNPs exhibited strong antibacterial activity against Gram-negative bacteria [22]. *Cardaria draba (L.)* was collected in July 2023 at approximately 2000 meters altitude and 39°54′0″N 41°15′0″E coordinates in Erzurum (Turkey), and silver nanoparticles were obtained from the aboveground parts. In our study, AgNPs were synthesized biologically using the aboveground parts of the *C. draba* plant. Characterization was performed with UV-Vis, XRD, FT-IR and SEM analyses. In addition to examining the antibacterial activities of AgNPs, enzyme inhibition on some enzymes of medical importance was examined. The cytotoxicity of the human colon cancer cell line (DLD-1) was investigated.

MATERIALS AND METHODS

Preparation of *Cardaria draba* L. Extract and Synthesis of Silver Nanoparticles

The aboveground parts of the plant were collected, washed thoroughly with pure water twice, dried, and ground thoroughly in a porcelain mortar. Thirty grams of ground plant parts were mixed in 100 mL of deionized water, with a magnetic stirrer for 30 minutes. Then, it was heated in a water bath at 60°C for 10 minutes. After cooling to room temperature, it was centrifuged at 3500 rpm for 10 minutes and filtered through filter paper to obtain the plant extract [23]. Synthesis of silver nanoparticles was carried out similarly to the working procedures of Manosalva et al (2019) [24]. To obtain silver nanoparticles, 20 mL of plant extract was added dropwise to 100 mL of 1 mmol (0.170 g) AgNO3 solution using a dropping funnel. The reaction continued for 2 hours at 50°C in a magnetic stirrer. The light yellow plant extract turned brown with the addition of silver nitrate solution. This brown colloidal solution was centrifuged at 10,000 rpm for 15 minutes to precipitate AgNPs. The AgNPs precipitated by centrifugation were washed several times with deionized water and then dried.

Characterization of Silver Nanoparticles

Ultra violet (UV-VIS) spectral analysis

Whether pure Ag+ ions were reduced was determined by UV-Vis spectral analysis. UV-vis spectra of biosynthesized AgNPs were determined in the wavelength range of 300-700 nm using a spectrophotometer (Agilent CARY 60 UV-visible spectrophotometer).

Scanning electron microscopy (SEM) analysis

It was characterized by scanning electron microscopy (SEM) (Tescan Maıa3 XMU) to determine morphology and the particle size.

X-ray diffraction (X-RD) analysis

The morphology of the crystal structure of AgNPs was analyzed by XRD (RIGAKU ULTIMA IV XRD) in the range of 3° to 79° for 2θ. The crystal size of AgNPs was calculated by using the Debye-Scherrer equation ($D=K\lambda/\beta \cos\theta$).

Fourier transform infra red spectroscopy (FT-IR) analysis

FT-IR (Perkin Elmer Spectrum 100 FTIR) spectroscopy analysis was performed to determine the functional groups present in the plant extract, as well as those playing a role in the reduction, in the range of 4000-400 cm-1 at the end of the reaction.

GC/MS (Gas chromotography/mass spectrometry) analysis

GC/MS analysis was performed according to Basar et al. (2024) [25].

Phenolic Component Analysis OF *C. draba* Extract by LC-MS/MS Method

LC-MS/MS analysis of the phenolic compound was performed using an Agilent 6460 Triple Quadrupole model (Agilent Technologies, Wilmington, DE, USA). The column temperature was fixed at 40 °C. The elution gradient was formed from mobile phase A (water, 0.1% Formic acid) and mobile phase B (acetonitrile with 0.1% formic acid). The mobile phase gradient was programmed as follows: 98% A (v/v) from 0 to 4.0 min, 98–80% A (v/v) from 4.0–7.0 min, 80–10% A (v/v) from 7.0–14.0 min, 10% A (v/v) from 14.0–15.0 min, 10–98% A (v/v) from 15.0–17.0 min. The total run time was 17 min, and the column equilibration time between each run was 4 min [26].

Antibacterial Activity

Antibacterial activity was determined by working on Gram negative (*Escherichia coli* ATCC 25922, *P. aeruginosa* ATCC 27853, *A. baumannii* ATCC 17978) and Gram positive (*Bacillus cereus* DSSM 4312, *S. aureus* ATCC 25923, *E. faecalis* ATCC 29212) bacteria. The disk diffusion method was used to determine antibacterial activity (NCCLS 1997). Nutrient broth liquid medium, which was inoculated with each microorganism using loop inoculation, was incubated for 12-16 hours at 37 °C. 100 µl sample of the test microorganisms, prepared from an overnight culture, was taken and spread on nutrient agar solid medium. Then, 10 µl of different concentrations of all extracts were taken and absorbed onto sterile paper disks, which were placed in petri dishes, and the spread was made. Inhibition zone diameters were measured after 24 hours, of incubation at 37 °C for bacteria. The same procedure was repeated for positive (Chloramphenicol) and negative controls (ethanol and water). Each test was performed in three replicates at different times [27].

Enzyme Inhibition

Antiurease and anticollagenase enzyme inhibition were performed according to Bakır and Kurbanoglu (2022) [28]. Lipoxygenase (LOX) enzyme inhibition was performed according to Bakır et al. (2022) [29].

RESULTS AND DISCUSSION

SEM Analysis

Figure 1 illustrates the scanning electron microscopy (SEM) images of silver nanoparticles (AgNPs) produced via the green synthesis process using *C. draba*. It is evident from the SEM images that the particles exhibit a range of sizes. Silver nanoparticles were discovered to have spherical shapes with an average diameter of 41 nm. From the SEM images, it can be observed that the silver nanoparticles are larger than expected as a result of a series of reactions triggered by the evaporation of the solvent due to the aggregation of the nanoparticles during sample preparation. This may have caused the differences in particle size [30]. The size of the particles was found to be 30-70 nm in the SEM study of AgNPs generated from *Vitis vinifera* (grape) fruit [31]. According to studies by Shah et al. (2018) on *Daphne mucronata* and Santhoshkumar et al. (2017) on *Gnidia glauca*, a species in the Thymelaeaceae family, silver nanoparticles have a spherical shape [32, 33]. The size and surface charge of the synthesized particles have an important effect on the interaction with the cells. Accordingly, when establishing the optimal conditions, the criteria exhibiting the smallest values for these parameters in the synthesized nanoparticles were selected.

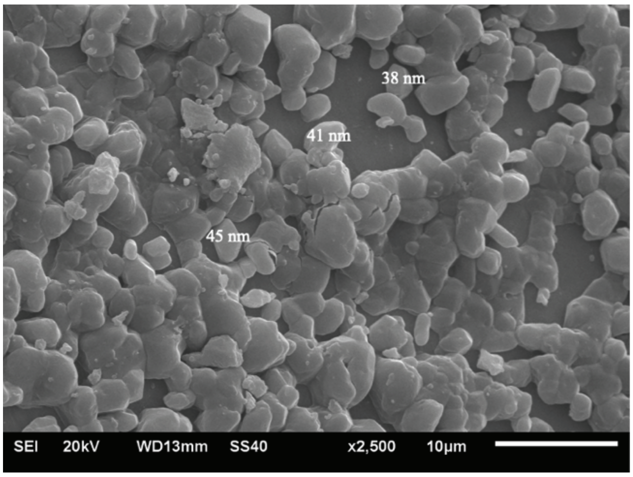

Figure 1. Images of SEM analyze of synthesized silver nanoparticles.

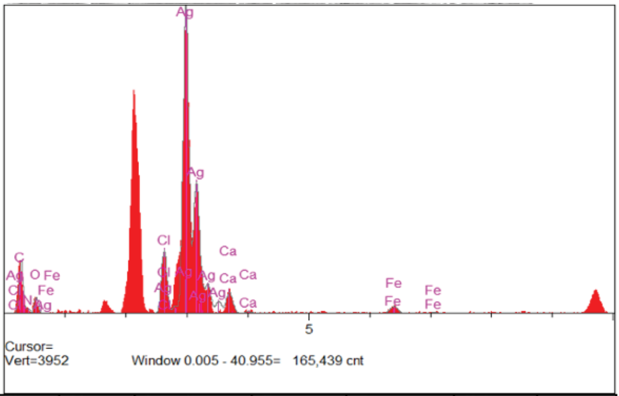

Elt.	Line	Intensity (c/s)	Error 2-sig	Conc	Units	
C	Ka	138.68	4.299	8.800	wt.%	
N	Ka	10.83	1.853	4.901	wt.%	
O	Ka	38.24	2.899	1.737	wt.%	
Cl	Ka	163.52	5.938	3.053	wt.%	
Ca	Ka	71.72	4.579	2.008	wt.%	
Fe	Ka	34.75	3.456	1.381	wt.%	
Ag	La	1,123.31	11.466	78.119	wt.%	
				100.000	wt.%	Total

Figure 2. EDX result of nanoparticles.

EDX Analysis

As illustrated in Figure 2, the elemental composition of the AgNPs produced at room temperature was determined to be 78.11 % Ag, 8.8 % C, 4.9 % N, 3.05 % Cl, 2.00 % Ca and 1.38 % Fe . The strong peaks of the formed AgNPs in an optical absorption band at 3 eV indicate the presence of silver within the particles. It indicates that AgNPs are dense. At the same time, it was determined that some elements other than silver also formed weak peaks. In another study, it was reported that nanoparticles obtained from *Salvia officinalis* (Sage) plant contained 60.97% silver [34]. AgNPs synthesized from *Murraya koenigii* (Curry) plant were found as 60% Ag, 19% C, 12% O, and 6% Cl [35]. Also, the EDX spectrum shows the presence of Cl, N, O, K, and C atoms in different percentages. Weak signals such as chlorine, carbon, and oxygen in the EDX profile are caused by phytochemicals found on the surface of the nanoparticles. Bacteria have the genetic ability to transmit and acquire drug resistance to therapeutic drugs. Resistant bacteria pose a challenge in the treatment of various well-known infections and require new substances with antimicrobial properties. The composition of the remaining substances in EDX and their effects on antimicrobial purposes may have implications.

FT-IR Analysis

FT-IR analyses show that AgNPs are surrounded by biomolecules, reducing the potential for metal nanoparticles to come together and form clusters, and increasing their stability in the solution environment. The peaks in the FT-IR spectrum of *C. draba* plant extract indicate the presence of 3675.83 -OH and -NH (polyphenols and amine) groups. The peaks at 2988.26 and 2901.60 cm^{-1} indicate the presence of –CH and -CH2 aliphatic groups, and the peaks at 1056.84 and 1028.01 cm^{-1} indicate the presence of -C-O groups, namely terpenoids, flavones, and carbohydrate structures (Fig. 3). It has been reported that FT-IR peaks in plant extract support the presence of antioxidant flavonoids and phenolic acids, and the presence of phenolics in the extract may be responsible for the reduction of metal ions and the formation of nanocomposites [36]. It was observed that AgNPs showed absorption peaks at 3675.72, 2988.77, 1513.93, 1393.93, 1230.26, 1141.96, 1066.27 cm^{-1} (Fig. 3). The first peak is seen as a band around 3675 cm^{-1}. The peak observed in this region generally represents -OH (hydroxyl) groups. It shows that the AgNPs sample contains various organic functional groups and compounds. The presence of hydroxyl (-OH) and carbonyl (C=O) groups, in particular, suggests that there are water molecules, alcohol, a phenol, or aldehyde, or ketone, or other related compounds on the surface of the sample. The peak located around 1513 cm^{-1} represents the stretching vibrations of carbonyl (C=O) and C=C double-bonded groups. Carbonyl groups can be found in aldehyde, ketone, or amide groups and the peak in this wavenumber region suggests the presence of such functional groups in the sample [37]. A comparison of the extract and nanoparticle peaks in FTIR analysis, conducted using Cornelian cherry fruit for the synthesis of AgNP, revealed that the 3159 cm-1 O-H, 1717 cm-1 C=O, 1224 cm-1 C-OO groups were the primary contributors to Ag reduction [37]. According to the FTIR analysis results, the -OH group at 3332 cm-1, the -C≡N group at 2145 cm-1, and the -C=O group at 1635 cm-1 participate in the synthesis process of nanoparticles [38]. FT-IR analysis shows that AgNPs have a complex chemical structure; organic and inorganic components are present on their surface. May have a suitable profile for use in potential biomedical and chemical applications.

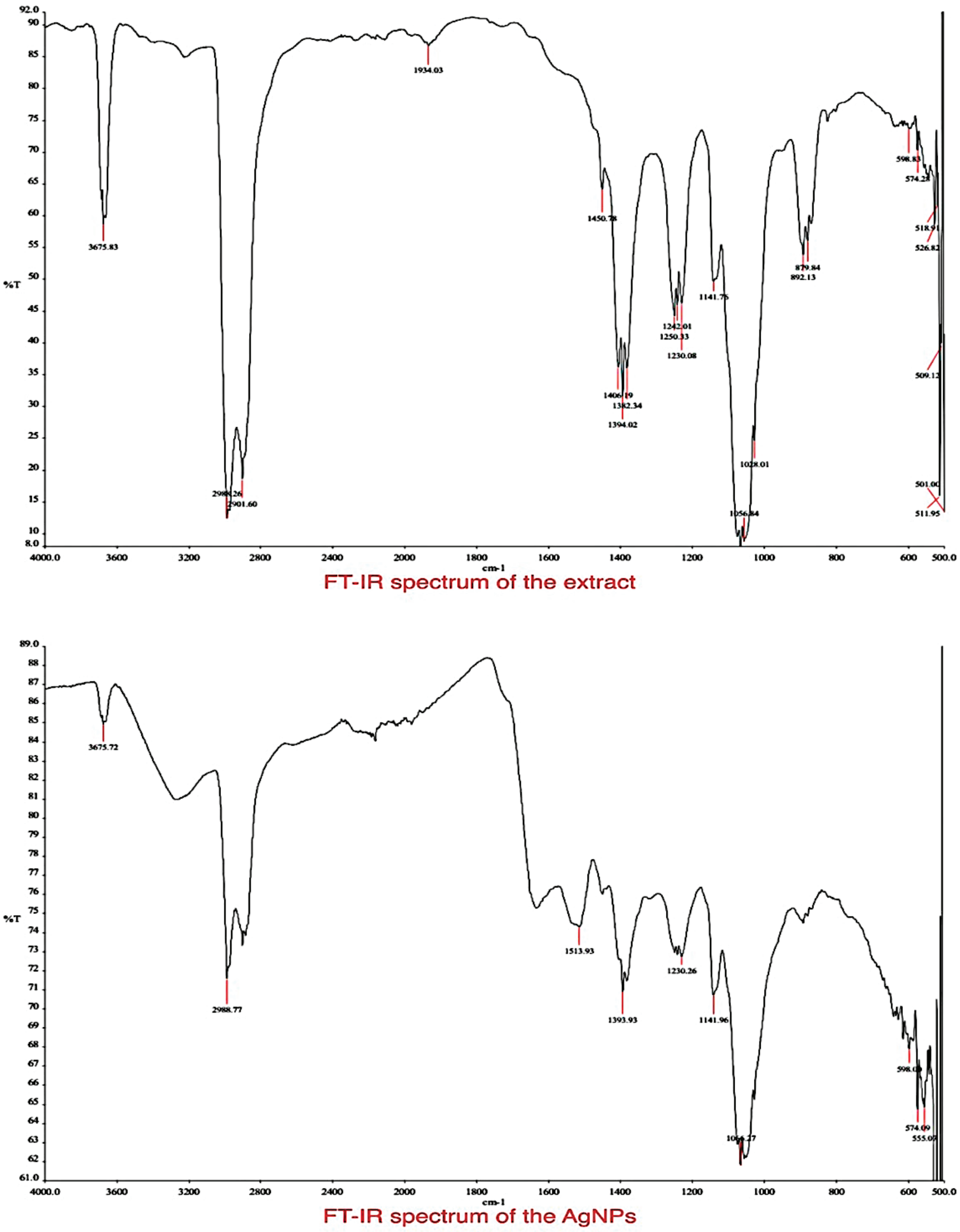

Figure 3. FT-IR result of extract and AgNPs.

XRD Analysis

Peaks from the (111), (200), (220), and (311) crystal structures were seen as a result of the resulting difraction patterns. These peaks corresponded to the angle values of 2θ=38.38°, 44.61°, 64.97°, and 78.09°, for metallic silver (JCPDS 04-0783) (Fig. 4). These findings led to the understanding that, in this context, a face-centered cubic structure contained metallic silver. Furthermore, the metals from the factory were identified as contaminants based on the difraction patterns. Using the Scherrer equation and the XRD data, the particle sizes of AgNPs were determined in this section of the study. The particle size of AgNP is 18.51 nm according to the Debye-Scherrer equation. According to Agarwal et al. (2018), who synthesized AgNPs from *Cymbopogon citratus*, the aforementioned peaks correspond to those of silver [39]. It was found that in *Nigellla sativa* plant, there were diffraction bands of (111), (200), (220) and (311) with 2ϴ values around 38.35°, 44.50°, 64.76° and 77.80° [40]. The sharpness of the peaks reveals that the synthesized nanoparticles have a high crystalline structure. In addition, the absence of peaks belonging to any other phase in the graph supports the high purity of the synthesized nanoparticles.

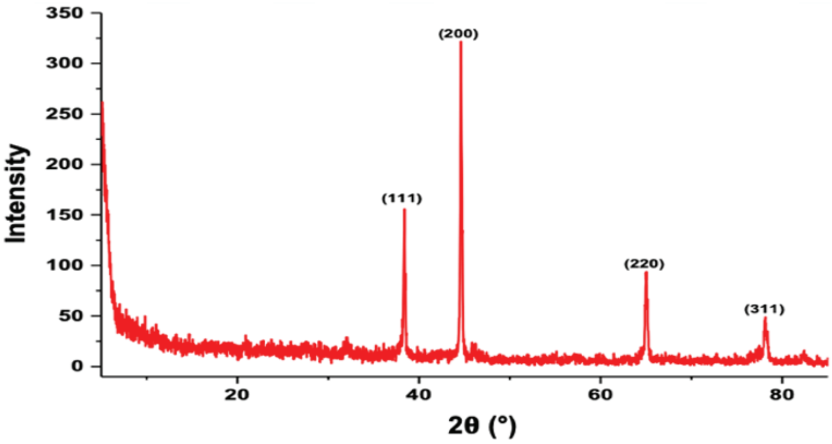

Figure 4. XRD result of nanoparticles.

UV-Visible Spectral Analysis

UV-Vis spectra of AgNPs synthesized from *C. draba* plants were taken. As seen in Figure 5, absorbance values are in the range of 400 to 500 nm. According to previous studies, the absorbance ranges of AgNPs generally occur at 400-500 nm. It has been reported that the transformation from a light yellow to brown colloidal solution during the reaction allows the qualitative detection of AgNPs. The color change is due to the plasmon resonances (SPR) on their surfaces and indicates an increase in the concentration of AgNPs over time. When literature findings are evaluated, they show that the synthesis was carried out successfully in the research.

This analysis confirmed the literature indicating that silver nanoparticles typically exhibit maximum absorption values at approximately 400 nm wavelength. AgNPs were synthesized with extracts obtained from *Rubus ellipticus*, and it was determined that the maximum absorbance value was obtained around 430 nm [41]. AgNPs were synthesized using *Punica granatum* extract. The maximum UV-vis absorbance value of the plant extract was determined to be 367 nm. The maximum UV-vis absorbance value of AgNPs was determined as 462 nm [42]. The greatest absorbance peak was observed in the range of 420–450 nm when AgNPs were produced from the *Salvia limbata* (sage) plant [43]. This finding substantiates the hypothesis that when exposed to the bioactive elements of the plant extract, the silver ion undergoes a transformation into silver nanoparticles [44].

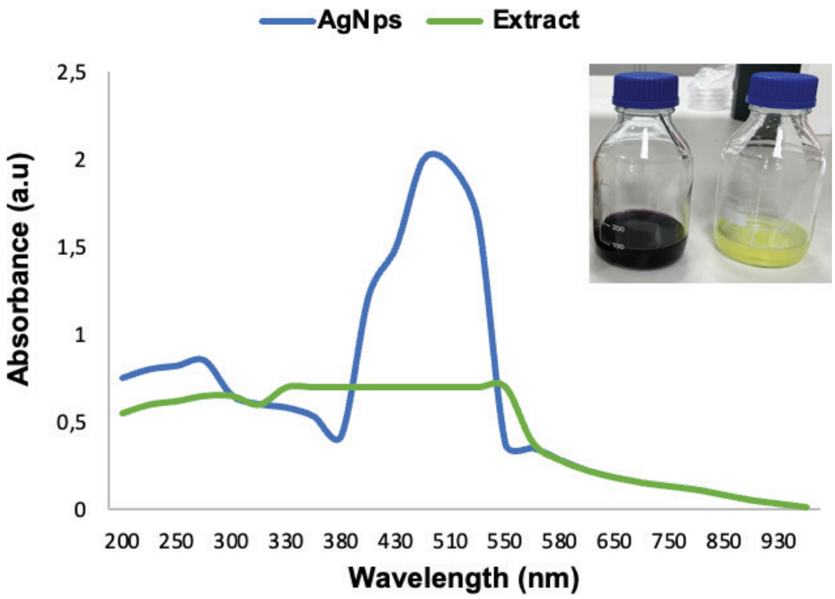

Figure 5. UV-Vis result of AgNPs and extract.

Gas Chromatography–Mass Spectrometry (GC/MS) Results

Gas chromatography-mass spectrometry (GC-MS) was used to analyze the essential oils obtained from the aerial part of the *C. draba* plant. The analysis revealed that the allyl isothiocyanate compound was responsible for 74.07 percent of the total weight of the plant extract. After the allyl isothiocyanate compound, thiocyanic acid, 2-propenyl ester compound, comprising 8.45 percent of the weight, constituted a significant part of the plant extract . Other components in the extract were less than 2 percent of the total extract weight (Table 1). Chemical analysis of *C. draba* flower, leaf, stem, and root sections gathered from Iran revealed that 6-10, 14-Trimethyl-2-pentadecanone (16.4%) and 3-butenyl isothiocyanate (26.4%) were the most prevalent components [45]. Chemical analysis of *C. draba* aerial organs and leaves obtained from France revealed that 6,10,14-trimethyl-2-pentadecanone (20.61%) and (E)-phytol (11.38%) were the most significant components [46]. *C. draba* roots, stems, leaves, flowers, and fruits gathered from Tunisia were examined for their primary fragrance volatiles, which included hexadecanoic acid (34.6%), 6-methyl-5-hepten-2-one (18.3%), decanal (15.0%), 6,10,14-trimethyl-2-pentadecanone (13.2%), and n-pentacosane (13%) [47].

Liquid Chromatography–Mass Spectrometry (LC-MS/MS) Results

In the LC-MS/MS results of the *C. draba*, Vitexin compound is the phenolic compound found in the highest amount with 8561.6281 ng/mL. Luteolin is the second most abundant phenolic compound after Vitexin. Rosmarinic acid, which has a large amount of reactive functional groups, was found at a concentration of 1.0837 ng/mL. Further data on other reactive phenolic compounds can be reviewed in Table 2. Since the focus was on the most abundant compounds in the plant extract, seven compounds are included in Table 2.

Antibacterial Activity

In the study, the paper disc method was used to examine the antibacterial activity of *Cardaria draba* extract and AgNPs biologically generated from *Cardaria draba* extract. The antibacterial impact of the extract on both Gram-positive and Gram-negative bacteria, including *B. subtilis, S. aureus*, and *E. faecalis was investigated* The antimicrobial activity tests yielded an inhibitory zone of 18–30 mm generated by chloramphenicol antibiotic discs in Petri dishes, which served as positive controls. The aqueous extract of *Cardaria draba* demonstrated a significant bactericidal effect on both Gram-negative and Gram-positive bacteria, with zones of inhibition ranging from 6 mm to 9 mm. The most effective antibacterial dose against *P. aeruginosa* was 9 (Fig. 6). For *S. aureus* ATCC 25923 and *E. faecalis* ATCC 29212, AgNPs showed an inhibitory zone for the bacteria *E. coli* ATCC 25922, *P. aeruginosa* ATCC 27853, *B. subtilis* DSMZ 1971, and *S. enteritidis* ATCC 13075 (Table 3).

When the antibacterial activity of silver nanoparticles synthesized from *Trema orientalis* (L.) was examined, it was found that silver nanoparticles formed a 9 mm zone at a concentration of 25 μg/mL, for *S. aureus* [48]. The antibacterial activity of silver nanoparticles synthesized using Ferula gummosa essential oil against Gram-positive and Gram-negative bacteria was shown with inhibition zones of 10 mm and 8 mm in diameter for *E. coli* and *S. aureus*, respectively [49]. In the antibacterial activity of silver nanoparticles made from *Mirabilis jalapa* leaf extract, *Staphylococcus aureus* showed a 10 ± 1.58 mm inhibition zone, *Pseudomonas aeruginosa* showed a 6 ± 1.15 mm inhibition zone, and Staphylococcus aureus AgNPs showed a 10 ± 1.58 mm inhibition zone [50]. Inhibition was observed in

Table 1. Biologically active chemical compounds of *Cardaria draba* aqueous extract

Name of compounds (molecular formula)	Retention time, min	%
Allyl Isothiocyanate	13.999	74.07
Thiocyanic acid, 2-propenyl ester	16.915	8.45
Silane, ethenylethoxydimethyl-	35.281	2.77
Benzaldehyde (CAS)	19.049	1.45
Isobutyl isothiocyanate	12.498	1.33
Alpha-Terpineol	24.519	1.20
Ethanone, 1-(1,3a,4,5,6,7-hexahydro-4-hydroxy-3,8-dimethyl-5-azulenyl)-	32.412	0.66
Cyclobutanol (CAS)	0.019	0.59
Propanoic acid, 2-methyl-, 3-hydroxy-2,4,4-trimethylpentyl ester	29.104	0.54
Benzeneethanol (CAS)	30.157	0.49
2,2,4-Trimethyl-1,3-pentanediol diisobutyrate	29.413	0.47
Cycloheptasiloxane, tetradecamethyl-	19.569	0.45
trans-.beta.-Ionone	30.768	0.43

Table 2. Most abundant phenolic compounds in quantitative analysis results

Molecule name	Structure	Final cons. (ng/mL)
Vitexin	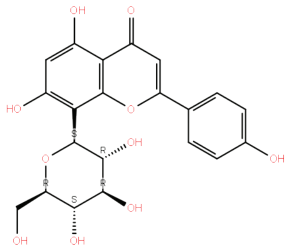	8561.6281
Luteolin	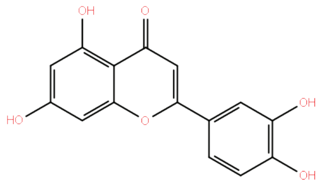	569.0751
Cyanidin-3-o-glucoside	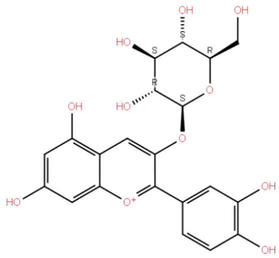	446.8699
Apigenin	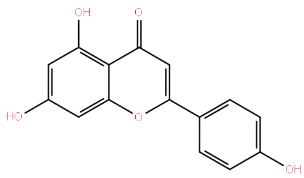	108.6049
Quercetin	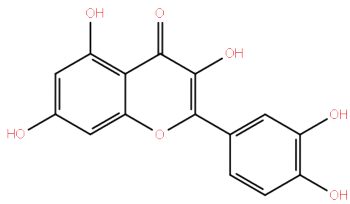	60.4772
Isorhamnetin	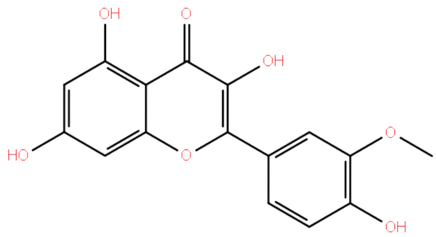	58.1453
Rosmarinic Acid	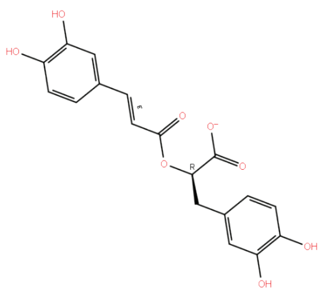	1.0837

Table 3. Zone diameters (in mm) and mean ± SE values of AgNPs' effects against bacterial strains, as determined by the disk diffusion method, are given in the table

Bacterial isolates	AgNPs (mm)	Chloramphenicol
B. cereus (ATCC 11778)	6.6±1.23	17 mm
S. aureus (ATCC 25923)	8.3±0.3	18 mm
E. faecalis (ATCC 29212)	5±0.5	17 mm
P. aeruginosa (ATCC 27853)	6.8±0.0	18 mm
E. coli (ATCC 25922)	7±0.0	17 mm
A. baumannii (ATCC 17978)	5.6±0.3	18 mm

the antibacterial effect of silver nanoparticles formed with the aqueous extract of *Aquilegia pubiflora* against *E. coli* (10.9 ± 0.29), *B. subtilis* (10.2 ± 0.31), *Klebsiella pneumoniae* (9.8 ± 0.33), *S. epidermidis* (9.3 ± 0.37), and *P. aeruginosa* (9.1 ± 0.34) [51]. The antibacterial impact of *C. draba* may be linked to the presence of phenolic chemicals, which have demonstrated antimicrobial action. The antibacterial activity of Brassicaceae members against clinical bacterial isolates was examined by Panghal [52]. The generally higher antibacterial activity of AgNPs may be due to the large surface area of nanoparticles, which provides better contact with microorganisms. According to the literature, the precise mechanism of AgNPs remains unclear. AgNPs have antibacterial properties because they create pits in bacterial cell walls [53].

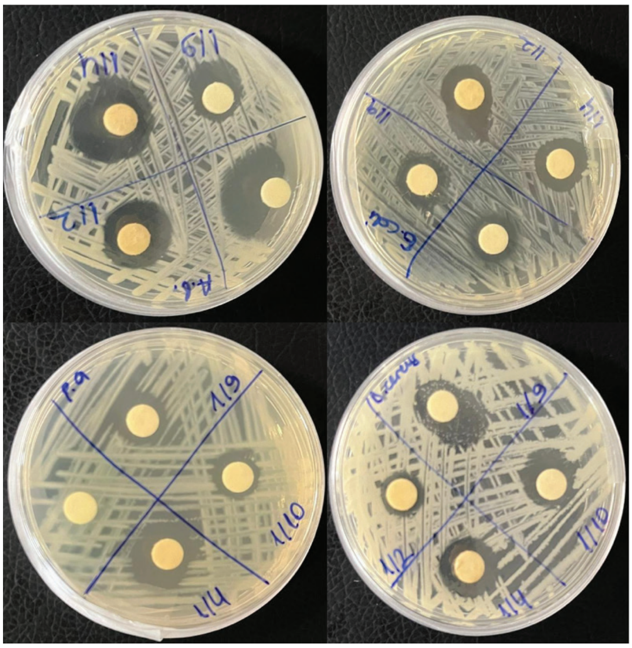

Figure 6. a) Zone diameters of AgNPs against Gram-negative bacteria, b) Zone diameters of AgNPs against Gram-positive bacteria.

Enzyme Inhibition

To observe the inhibitory effects of *C.draba* extract and AgNPs synthesized from it, tests were performed on three different enzymes: urease, collagenase, and lipoxygenase. Percentage inhibition and IC_{50} values were determined.

Effect on Urease

The urease inhibition test demonstrated significant inhibitory effects of *C. draba* extract and AgNPs. C. draba extract showed 34.44% (IC_{50}: 2.60± 1.32 µg/mL) inhibition at 2 µg/mL concentration. AgNPs showed 44.64% (IC_{50}: 2.23± 1.65 µg/mL) inhibition at the same concentration. AgNPs produced with *C. draba* extract showed strong inhibitory activity against urease. Thiourea, when used as a positive control, showed strong inhibition of 57.77% (Table 4). Ovais et al. evaluated the capacity of the green synthesis of AgNPs to inhibit urease enzyme activity using *Olax nana* Wall. ex *Benth.* AgNPs showed significant inhibitory activity with a urease inhibition of 39.23 ± 0.42% at a concentration of 0.2 mg/mL [54]. In the study conducted by Kaya et al., when *Thymbra spicata* L subsp. *spicata* L was tested at a concentration of 100 µg/mL, urease enzyme inhibition was observed, reducing its activity by 34.62±2.33%, [55]. AgNPs and AuNPs were synthesized with *Crataegus oxyacantha* extract. Among the synthesized nanoparticles, AgNPs showed inhibitory activity with an IC_{50} value of 1.38 ± 0.3 µM. The −NH, −OH, and C=O groups of the stabilizing phytochemicals, which interact with Ni in the urease enzyme, may be the cause of the notable urease inhibitory actions of NPs [56].

Effect on Collagenase

Collagenase inhibition test showed significant inhibitory effects of *C. draba* extract and AgNPs. *C. draba* extract showed 12.59% inhibition at a 2 µg/mL concentration. AgNPs showed 35.55% inhibition at the same concentration. AgNPs produced with *C. draba* extract showed strong inhibitory activity against collagenase. EGCG (Epigallocatechin gallate), used as a positive control, showed 48.14% inhibition (Table 4). In the study by Kaya et al., *Thymbra spicata* L. subsp. *spicata* L. was determined to exhibit a low collagenase enzyme inhibitory activity (10.57±0.30%) [57]. Radwan et al.[58] stated that the nanoparticles they obtained inhibited the collagenase enzyme by an average of 75%. AgNPs obtained from *F. vesiculosus* have been shown to have stronger anti-collagenase activity than *F. vesiculosus* extract. Terpenoids and flavonoids, two naturally occurring antioxidants, work in concert to block the collagenase enzyme [59]. It may be claimed that various plant extracts are the source of bioactive compounds that can block the activity of the same enzymes, which is consistent with the findings of Andrade et al. (2021) [60] and Gomes et al. (2022) [61].

Effect on Lipoxygenase (LOX)

The lipoxygenase inhibition test showed significant inhibitory effects of *C. draba* extract and AgNPs. *C . draba* extract showed 27.40% inhibition at 2 μg/mL concentration. AgNPs showed 38.88% inhibition at the same concentration. AgNPs produced with *C .draba* extract showed strong inhibitory activity against lipoxygenase. Nordihydroguaiaretic acid (NDGA), used as a positive control, showed strong inhibition of 54.44% (Table 4). This study did not show any LOX enzyme inhibition activity. This study highlights the possible variation in enzyme inhibitory activity based on elements including the plant's particular composition, the plant material's place of origin, and the experimental setup.

Cytotoxicity Analysis

The cytotoxicity of AgNPs was investigated. Figure 7 illustrates the cell viability rates for the DLD-1 colorectal adenocarcinoma cell line when AgNPs was administered at varying concentrations (2500, 1250, 625, and 312.5 ppm). The lowest concentration of AgNPs applied in the study, when compared to the control group, was 312.5 ppm. The remaining applied concentrations were observed to exert a diminished cytotoxic effect. The lowest concentration in the AgNPs, that was found to be less cytotoxic than the control group, was determined to be 312.5 ppm. Furthermore, concentrations of 625 and 1250 ppm were demonstrated to be less cytotoxic than the specified threshold value. The human body's digestive system is capable of transporting nanoparticles into the bloodstream, where they can subsequently be delivered the liver, brain, and other organs. Nanoparticles have the potential to deliver therapeutic medications to the brain and other organs [62]. The decrease

Table 4. Enzyme inhibitory activity of extracts and AgNPs from *C. draba*

Enzyme	Tested samples	Concentrations	% inhibition	IC50
Urease	*C. draba*	2 μg/mL	34.44	2.60± 1.32 μg/mL
	AgNPs	2 μg/mL	44.64	2.23± 1.65 μg/mL
	Thiourea	2 μM	57.77	21.98 ± 1.01 μM
Collagenase	*C. draba*	2 μg/mL	12.59	2.14 ± 1.09 μM
	AgNPs	2 μg/mL	35.55	2.29 0.88 μg/mL
	EGCG (Epigallocatechin gallate)	2 μM	48.14	13.76± 0.64 μg/mL
Lipoxygenase (LOX)	*C. draba*	2 μg/mL	27.40	2.1 ± 0.88 μg/mL
	AgNPs	2 μg/mL	38.88	4.66 ± 0.00 μg/mL
	Nordihydroguaiaretic acid (NDGA)	2 μM	54.44	1.55 ± 0.64 μM

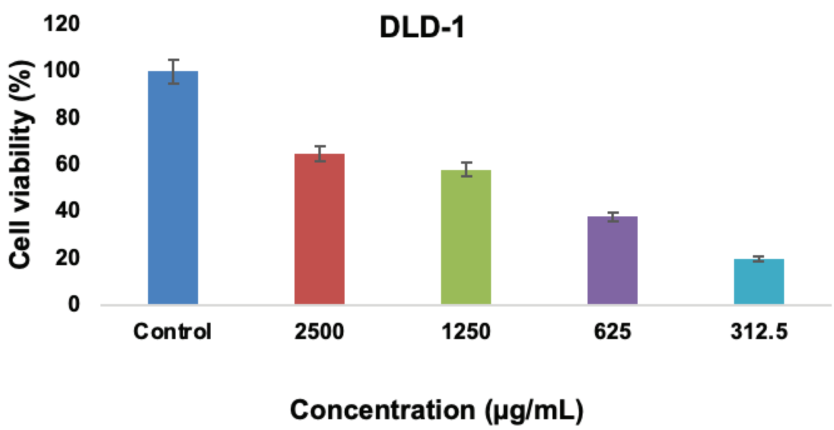

Figure 7. The effect of AgNPs on colorectal adenocarcinoma cell line DLD-1.

in cell viability rate compared to the administered dose indicates that AgNPs exert a cytotoxic effect on the DLD-1 cell line. Sivri et al. (2023) investigated the effects of ZnO nanoparticles using *Laurus nobilis* leaf extract in DLD-1 and L929 cell lines. They found that the nanoparticles were only effective in the DLD-1 cell line and stated that they have the potential to be used in biomedical applications due to their antibacterial and anticancer activities [63]. Pillai et al. (2022) investigated the toxicity of iron oxide NPs in DLD-1 human colon cancer cells and normal L929 (fibroblast) cells. They showed significant cytotoxicity in DLD-1 cancer cell lines [64]. Bidian et al. (2023) showed that gold and silver nanoparticles obtained from *Cornus mas* fruit extract both protected normal cells and induced the death of DLD-1 tumor cells, particularly through apoptosis [65]. El-Bahr et al. (2021) investigated the healing effects of iron oxide nanoparticles prepared from *Petroselinum crispum* leaf extract in anemic rats and showed that they can be used as an effective treatment [66].

CONCLUSION

In this study, AgNPs were produced using a straightforward, inexpensive, rapid, and environmentally friendly biosynthetic approach, employing fresh *C. draba* as the source material. The antibacterial properties of the substance have been investigated in relation to various infectious microorganisms. It has been observed that the nanoparticles obtained from these plants have an inhibitory effect on the nosocomial infection agents *E. coli, Staphylococcus aureus, Acinetobacter baumannii, Pseudomonas aeruginosa,* and *Enterobacter* species, which have multiple antibiotic resistance. We think that AgNPs may provide an alternative solution in the treatment of infectious diseases due to their broad-spectrum antibacterial activity, supported by optimization studies. The MTT method was employed for the determination of anticancer activity using a colorectal adenocarcinoma cell line. Test results revealed significant cytotoxicity. In addition to its antibacterial and anticancer effects, it is a good source of molecules effective against urease and collagenase. It is also suggested that the plant samples used may serve as efficacious biological agents when all the data are taken into account, and they can be developed and used in the treatment of various diseases.

AUTHORSHIP CONTRIBUTIONS

Authors equally contributed to this work.

DATA AVAILABILITY STATEMENT

The authors confirm that the data that supports the findings of this study are available within the article. Raw data that support the finding of this study are available from the corresponding author, upon reasonable request.

CONFLICT OF INTEREST

The author declared no potential conflicts of interest with respect to the research, authorship, and/or publication of this article.

ETHICS

There are no ethical issues with the publication of this manuscript.

STATEMENT ON THE USE OF ARTIFICIAL INTELLIGENCE

Artificial intelligence was not used in the preparation of the article.

REFERENCES

[1] Zayed MF, Mahfoze RA, El-Kousy SM, Al-Ashkar E. In-vitro antioxidant and antimicrobial activities of metal nanoparticles biosynthesized using optimized Pimpinella anisum extract. Colloids Surf A Physicochem Eng Asp 2020;585:124167. [CrossRef]

[2] Chahar HS, Corsello T, Kudlicki AS, Komaravelli N, Casola A. Respiratory syncytial virus infection changes cargo composition of exosome released from airway epithelial cells. Sci Rep 2018;8:1–18. [CrossRef]

[3] Hussain I, Singh NB, Singh A, Singh H, Singh SC. Green synthesis of nanoparticles and its potential application. Biotechnol Lett 2016;38:545–560. [CrossRef]

[4] Geraldes AN, da Silva AA, Leal J, Estrada-Villegas GM, Lincopan N, Katti KV, et al. Green nanotechnology from plant extracts: synthesis and characterization of gold nanoparticles. Adv Nanoparticles 2016;5:176–185. [CrossRef]

[5] Shahidi F, Ho C. Phenolics in foods and natural health products: An overview. ACS Symp Ser 2005. [CrossRef]

[6] Vijayakumar S, Malaikozhundan B, Shanthi S, Vaseeharan B, Thajuddin N. Control of biofilm forming clinically important bacteria by green synthesized ZnO nanoparticles and its ecotoxicity on Ceriodaphnia cornuta. Microb Pathog 2017;107:88–97. [CrossRef]

[7] Kanakalakshmi A, Janaki V, Shanthi K, Kamala-Kannan S. Biosynthesis of Cr (III) nanoparticles from electroplating wastewater using chromium-resistant *Bacillus subtilis* and its cytotoxicity and antibacterial activity. Artif Cells Nanomed Biotechnol 2017;45:1304–1309. [CrossRef]

[8] Şahin M, Gübbük İH. Synthesis of antioxidant silver nanoparticles, characterization and catalysis Applications. Int J Adv Eng Pure Sci 2019;31:75–83. [CrossRef] [Turkish]

[9] Doğan Y, Başlar S, Mert HH, Ay G. The use of wild edible plants in Western and Central Anatolia (Turkey). Econ Bot 2004;58:684–690. [CrossRef]

[10] Şimşek I, Aytekin F, Yeşilada E, Yıldırımlı Ş. An ethnobotanical survey of the Beypazarı, Ayaş and Güdül district towns of Ankara Province (Turkey). Econ Bot 2004;58:705–720. [CrossRef]

[11] Akgül A. Midyat (Mardin) civarında etnobotanik. Yüksek Lisans Tezi, Ege Üniversitesi, Fen Bilimleri Enstitüsü, Biyoloji Anabilim Dalı, İzmir; 2008.

[12] Ertuğ F. An ethnobotanical study in Central Anatolia (Turkey). Econ Bot 2000;54:155–182. [CrossRef]

[13] Mart S. Bahçe ve Hasanbeyli (Osmaniye) halkının kullandığı doğal bitkilerin etnobotanik yönden araştırılması. Yüksek Lisans Tezi, Çukurova Üniversitesi Fen Bilimleri Enstitüsü, Biyoloji Anabilim Dalı, Adana; 2006.

[14] Erol MK, Tuzlacı E. Turkish folk medicinal plants. Part II: Eğirdir (Isparta). Fitoterapia 1999;70:593–610. [CrossRef]

[15] Radonić I, Blažević J, Mastelić M, Zekić M, Skočibušić A, Maravić, Phytochemical analysis and antimicrobial activity of *Cardaria draba* (L.) Desv. volatiles. Chem Biodivers 2011;8:1170–1181. [CrossRef]

[16] Naser EH, Khthr MFA, Abed SA. Phytochemistry and therapeutic uses of *Cardaria draba* L. Plant Arch 2019;19:118–125.

[17] Tuzlacı E, Erol MK. Turkish folk medicinal plants. Part II: Eğirdir (Isparta). Fitoterapia 1999;70:593–610. [CrossRef]

[18] Desv L, Bayan Y. Chemical composition and antifungal activity of the plant extracts of Turkey *Cardaria draba*. Egypt J Biol Pest Control 2016;26:579–581

[19] Al-Khafaji NMS, Al-Marzoqi AH, Hussein HJ. Influence of the crude phenolic, alkaloid and terpenoid compounds extracts of *Cardaria draba* (Lepidium draba L.) on human pathogenic bacteria. Eur J Botany Plant Sci Phytol 2016;3:15–19.

[20] Sharifi-Rad J, Hoseini-Alfatemi M, Sharifi-Rad JAT, Silva JD, Rokni M, Sharifi-Rad M. Evaluation of biological activity and phenolic compounds of *Cardaria draba* (L.) extracts. J Biol Today's World 2015;4:180–189. [CrossRef]

[21] Aktepe N, Baran A, Atalar MN, Baran MF, Keskin C, Taşkin A, Yavuz Ö, Demirtaş İ, Oğuz E, Jahan I. Analysis of bioactive compounds using LC–ESI–MS/MS, cytotoxic, antimicrobial effects, and enzyme activities from *Cyclotrichium origanifolium*. Chem Biol Drug Des 2023;101:740–748. [CrossRef]

[22] Farahani AF, Hamdi SMM, Mirzaee A. GC/MS analysis and phyto-synthesis of silver nanoparticles using *Amygdalus spinosissima* extract: Antibacterial, antioxidant effects, anticancer and apoptotic effects. Avicenna J Med Biotechnol 2022;14:223. [CrossRef]

[23] Antony JJ, Nivedheetha M, Siva D, Pradeepha G, Kokilavani P, Kalaiselvi S, Sankarganesh A, Balasundaram A, Masilamani V, Achiraman S. Antimicrobial activity of *Leucas aspera* engineered silver nanoparticles against *Aeromonas hydrophila* in infected *Catla catla*. Colloids Surf B Biointerfaces 2013;109:20–24. [CrossRef]

[24] Manosalva N, Tortella G, Diez MC, Schalchli H, Seabra AB, Durán N. Green synthesis of silver nanoparticles: effect of synthesis reaction parameters on antimicrobial activity. World J Microbiol Biotechnol 2019;35:88. [CrossRef]

[25] Başar Y, Yenigün S, Gül F, Özen T, Demirtaş İ, Alma MH, Temel S. Phytochemical profiling, molecular docking and ADMET prediction of crude extract of *Atriplex nitens* Schkuhr for the screening of antioxidant and urease inhibitory. Int J Chem Technol 2024;8:62–71. [CrossRef]

[26] Seraglio SKT, Valese AC, Daguer H, Bergamo G, Azevedo MS, Gonzaga LV, Costa ACO. Development and validation of a LC–ESI–MS/MS method for the determination of phenolic compounds in honeydew honeys with the diluted-and-shoot approach. Food Res Int 2016;87:60–67. [CrossRef]

[27] Hudzicki J. Kirby-Bauer disk diffusion susceptibility test protocol. Am Soc Microbiol 2009;15:55–63.

[28] Bakır Ö, Kurbanoğlu EB. Investigation of antioxidant activity and antiurease, anticollagenase enzyme inhibition profile of oleaster seeds. Int J Life Sci Biotechnol 2022;5:213–224. [CrossRef]

[29] Bakır Ö, Güller P, Kurbanoğlu EB. Synthesis, characterization, antibacterial, antioxidant activity, and lipoxygenase enzyme inhibition profile of silver nanoparticles (AgNPs) by green synthesis from *Seseli resinosum* Freyn & Sint. Int J Plant-Based Pharm 2022;2:182–189. [CrossRef]

[30] Ramirez-Acosta CM, Cifuentes J, Cruz JC, Reyes LH. Patchy core/shell, magnetite/silver nanoparticles via green and facile synthesis, routes to assure biocompatibility. Nanomaterials 2020;10:9. [CrossRef]

[31] Hashim N, Paramasivam M, Tan JS, Kernain D, Hussin MH, Brosse N, Gambier F, Raja PB. Green mode synthesis of silver nanoparticles using *Vitis vinifera*'s tannin and screening its antimicrobial activity/apoptotic potential versus cancer cells. Mater Today Commun 2020;25:101511. [CrossRef]

[32] Shah A, Lutfullah G, Ahmad K, Khalil AT, Maaza M. *Daphne mucronata*-mediated phytosynthesis of silver nanoparticles and their novel biological applications, compatibility and toxicity studies. Green Chem Lett Rev 2018;11:318–333. [CrossRef]

[33] Santhoshkumar J, Rajeshkumar S, Venkat Kumar S. Phyto-assisted synthesis, characterization and applications of gold nanoparticles – A review. Biochem Biophys Rep 2017;11:46–57. [CrossRef]

[34] Okaiyeto K, Hoppe H, Okoh AI. Plant-based synthesis of silver nanoparticles using aqueous leaf extract of *Salvia officinalis*: characterization and its antiplasmodial activity. J Cluster Sci 2021;32:101–109. [CrossRef]

[35] Qais FA, Shafiq A, Khan HM, Husain FM, Khan RA, Alenazi B, Alsalme A, Ahmad I. Antibacterial effect of silver nanoparticles synthesized using *Murraya koenigii* (L.) against multidrug-resistant pathogens. Bioinorg Chem Appl 2019;1:11. [CrossRef]

[36] Atarod M, Nasrollahzadeh M, Sajadi SM. Euphorbia heterophylla leaf extract mediated green synthesis of Ag/TiO2 nanocomposite and investigation of its excellent catalytic activity for reduction of variety of dyes in water. J Colloid Interface Sci 2016;462:272–279. [CrossRef]

[37] Keskin M. Waste corn silk for eco-friendly silver nanoparticles: Green synthesis, characterization and determination of enzyme inhibition properties. J Serb Chem Soc 2025;90:369–382. [CrossRef]

[38] Aktepe N, Erbay N, Baran A, Baran M, Keskin C. Synthesis, characterization, and evaluation of the antimicrobial activities of silver nanoparticles from *Cyclotrichium origanifolium* L. Int J Agric Environ Food Sci 2022;6:426–434. [CrossRef]

[39] Filip GA, Moldovan B, Baldea I, Olteanu D, Suharoschi R, Decea N, Cismaru CM, Gal E, Cenariu M, Clichici S, David L. UV-light mediated green synthesis of silver and gold nanoparticles using Cornelian cherry fruit extract and their comparative effects in experimental inflammation. J Photochem Photobiol B Biol 2019;191:26–37. [CrossRef]

[40] Agarwal UP, Ralph SA, Reiner RS, Hunt CG. Production of high lignin-containing and lignin-free cellulose nanocrystals from wood. Cellulose 2018;25:5791–5805. [CrossRef]

[41] Karakaya Y, Janbazi H, Wlokas I, Levish A, Winterer M, Kasper T. Experimental and numerical study on the influence of equivalence ratio on key intermediates and silica nanoparticles in flame synthesis. Proc Combust Inst 2021;38:1375–1383. [CrossRef]

[42] Habib A, Bibi Y, Qayyum I, Farooq M. Hierarchical plant extracts in silver nanoparticles preparation: Minuscular survey to achieve enhanced bioactivities. Heliyon 2024;10:e24303. [CrossRef]

[43] Sahoo B, Panigrahi LL, Das RP, Pradhan AK, Arakha M. Biogenic Synthesis of Silver Nanoparticle from *Punica granatum* L. and Evaluation of Its Antioxidant, Antimicrobial and Anti-biofilm Activity. J Inorg Organomet Polym Mater 2022;32:4250–4259. [CrossRef]

[44] Nematollahi F. Silver nanoparticles green synthesis using aqueous extract of *Salvia limbata* CA Mey. Int J Biosci 2015;6:30–35. [CrossRef]

[45] Khane Y, Benouis K, Albukhaty S, Sulaiman GM. Green synthesis of silver nanoparticles using aqueous *Citrus limon* zest extract: Characterization and evaluation of their antioxidant and antimicrobial properties. Nanomaterials 2022;12:2013. [CrossRef]

[46] Eghbali S, Taleghani A, Moghimi R, Farhadi F, Hajizadeh M, Sarayan MS. Exploring the phytochemical and biological activity of *Cardaria draba*: Insights into Volatile and Nonvolatile Compounds. 2024;8:1170–1181. [CrossRef]

[47] Younes K, Merghache S, Djabou N, Selles C, Muselli A, Tabti B, et al. Chemical Composition and Free Radical Scavenging Activity of Essential Oils and Extracts of Algerian *Cardaria draba* (L.) Desv. J Essent Oil-Bear Plants 2015;18:1448–1458. [CrossRef]

[48] Saadellaoui W, Kahlaoui1 S, Hcini K, Haddada A, Sleimi N, Roberta. Profiles of the headspace volatile organic and essential oil compounds from the Tunisian *Cardaria draba* (L.) Desv. and Its leaf and stem epidermal micromorphology. Phyton-Int J Exp Bot 2024;93:725–744. [CrossRef]

[49] Das R, Kumar P, Singh AK, Agrawal S, Albukhaty S, Bhattacharya I, Al-aqbi ZT. Green synthesis of silver nanoparticles using *Trema Orientalis* (L.) extract and evaluation of their antibacterial activity. Green Chem Lett Rev 2025;18:2444679. [CrossRef]

[50] Valinezhad N, Talebi AF, Alamdari S. Biosynthesize, physicochemical characterization and biological investigations of chitosan-Ferula gummosa essential oil (CS-FEO) nanocomposite. Int J Biol Macromol 2023;241:124503. [CrossRef]

[51] Rauf S, Hameed H, Tariq M, Afareen A, Gulfaraz S, AlKubaisi NA, et al. Phytochemical-mediated synthesis and characterization of silver nanoparticles using *Mirabilis jalapa* leaf extract and their antibacterial. Microsc Res Tech 2025;88:1–11. [CrossRef]

[52] Jan H, Zaman G, Usman H, Ansir R, Drouet S, Gigliolo-Guivarc'h N, Abbasi BH. Biogenically proficient synthesis and characterization of silver nanoparticles (Ag-NPs) employing aqueous extract of *Aquilegia pubiflora* along with their in vitro antimicrobial, anti-cancer and other biological applications. J Mater Res Technol 2021;15:950–968. [CrossRef]

[53] Panghal M, Kaushal V, Yadav JP. In vitro antimicrobial activity of ten medicinal plants against clinical isolates of oral cancer cases. Ann Clin Microbiol Antimicrob 2011;10:21. [CrossRef]

[54] Kim SH, Lee HS, Ryu DS, Choi SJ, Lee DS. Antibacterial activity of silver-nanoparticles against *Staphylococcus aureus* and *Escherichia coli*. Microbiol Biotechnol Lett 2011;39:77–85.

[55] Ovais M, Khalil AT, Raza A, Islam NU, Ayaz M, Saravanan M, Ali M, Ahmad I, Shahid M, Shinwari ZK. Multifunctional theranostic applications of biocompatible green-synthesized colloidal nanoparticles. Appl Microbiol Biotechnol 2018;102:4393–4408. [CrossRef]

[56] Kaya EC, Akdeniz M, Ugurlu P, Yigitkan S, Toksoy MO, Firat M, Ertas A. Nanoparticle formation capacity and acaricidal effect (*Hyalomma marginatum*) of essential oil of *Thymbra spicata* L. subsp. spicata L. J Essent Oil-Bear Plants 2025;1-19.

[57] Ali S, Bacha M, Shah MR, Shah W, Kubra K, Khan A, et al. Green synthesis of silver and gold nanoparticles using *Crataegus oxyacantha* extract and their urease inhibitory activities. Biotechnol Appl Biochem 2021;68:992–1002. [CrossRef]

[58] Radwan RA, El-Sherif YA, Salama MM. A novel biochemical study of anti-ageing potential of *Eucalyptus camaldulensis* bark waste standardized extract and silver nanoparticles. Colloids Surf B Biointerfaces 2020;191:111004. [CrossRef]

[59] Savitri ES, Rahmawaty AE, Minarno EB. Antioxidant, anti-collagenase, and antibacterial activities of *Fucus vesiculosus* silver nanoparticles. Narra J 2024;4:e882. [CrossRef]

[60] Andrade JM, Domínguez-Martín EM, Nicolai M, Faustino C, Rodrigues LM, Rijo P. Screening the dermatological potential of *plectranthus* species components: Antioxidant and inhibitory capacities over elastase, collagenase and tyrosinase. J Enzyme Inhib Med Chem 2021;36:258–270. [CrossRef]

[61] da Costa Gomes A, Figueiredo CCM, Granero FO, Junior JLB, Ximenes VF, Silva LP, da Silva RMG. Antioxidant and antiglycation activities and inhibitory action of *Passiflora cincinnata* on collagenase, elastase and tyrosinase: in vitro and in silico study. Biocatal Agric Biotechnol 2022;44:102464. [CrossRef]

[62] Abudayyak M, Guzel E, Özhan G. Nickel oxide nanoparticles are highly toxic to SH-SY5Y neuronal cells. Neurochem Int 2017;108:7–14. [CrossRef]

[63] Sivri FM, Önem E, Akkoç S, Çırrık C, Ezer A. Biosynthesis of ZnO nanoparticles using *Laurus nobilis* leaf extract and investigation of antiproliferative and antibacterial activity potential. Int J Secondary Metabolite 2023;10:414–424. [CrossRef]

[64] Pillai RR, Sreelekshmi PB, Meera AP, Thomas S. Biosynthesized iron oxide nanoparticles: Cytotoxic evaluation against human colorectal cancer cell lines. Mater Today Proc 2022;50:187–195. [CrossRef]

[65] Bidian C, Filip GA, David L, Moldovan B, Olteanu D, Clichici S, Baldea I. Green synthesized gold and silver nanoparticles increased oxidative stress and induced cell death in colorectal adenocarcinoma cells. Nanomaterials 2023;13:1251. [CrossRef]

[66] El-Bahr SM, Elbakery AM, El-Gazzar N, Amin AA, Al-Sultan S, Alfattah MA, Hamouda AF. Biosynthesized iron oxide nanoparticles from *Petroselinum crispum* leaf extract mitigate lead-acetate-induced anemia in male albino rats: hematological, biochemical and histopathological features. Toxics 2021;9:123. [CrossRef]